Supporting Information

Aluminum-Enhanced Fluorescence of Cu_8 Nanoclusters: An Effective Method for Sensitive Detection of Fluoride in Aqueous and Bioimaging

Weihua Ding,[a] Lizhong Peng, [a] Damin Yun, [a] Sheng Gao, [a] Ruihong Duan, [b] Yayun Gu,[a] Chengniu Wang, [a] Wenqing Li, [a]* Xuhui Zeng,[a] Fei Sun [a]**

[a] Medical School, Institute of Reproductive Medicine, Nantong University, Nantong 226001, Jiangsu, China.

[b] College of Chemistry, Zhengzhou University, Zhengzhou 450001, Henan, China.

Corresponding author:

*E-mail: sunfei@ntu.edu.cn (Fei Sun),

*E-mail: dingweihua1988@163.com (Weihua Ding)

*E-mail: liwenqing505@163.com (Wenqing Li)

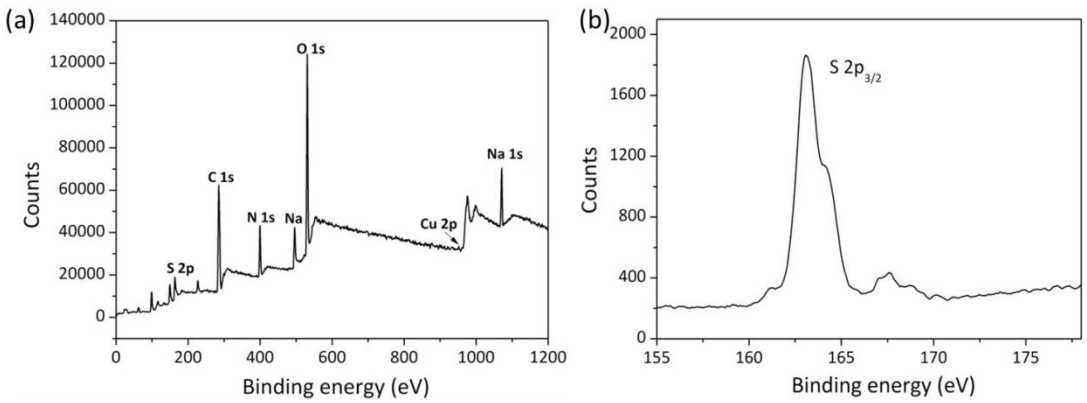

Figure S1. (a) XPS survey spectrum of the Cu NCs and (b) the expanded S 2p region.

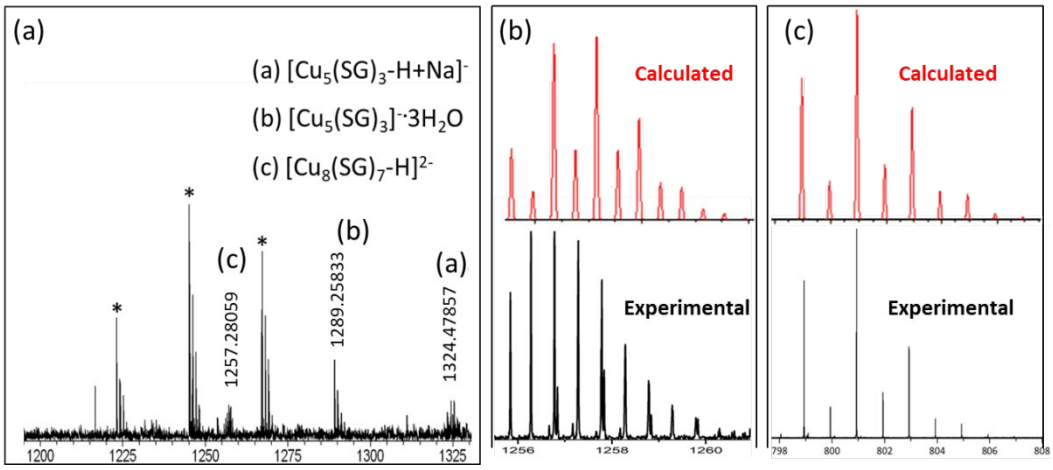

Figure S2. (a) The amplified ESI-MS of Cu NCs in the range of 1200-1350. The experimental and simulated isotopic pattern of (b) $[Cu_5(SG)_3\text{-}H+Na]^-$ (m/z=1257.28059) and (c) $[Cu_3(SG)_2\text{-}H]^-$ (m/z=800.92700). Asterisk (*) represents other miscellaneous peaks.

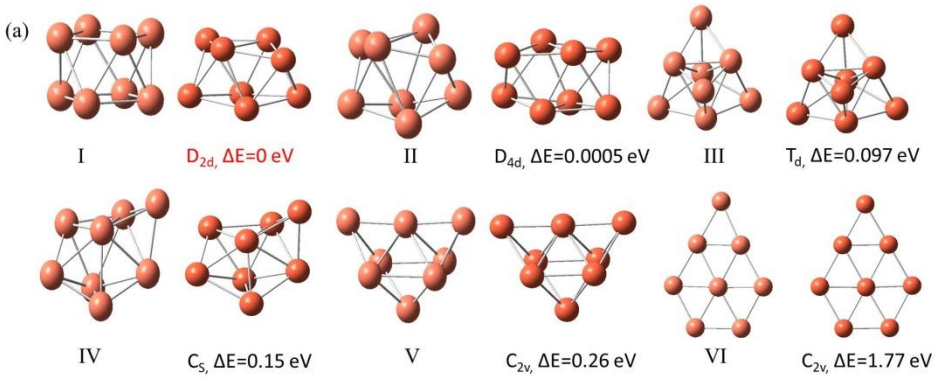

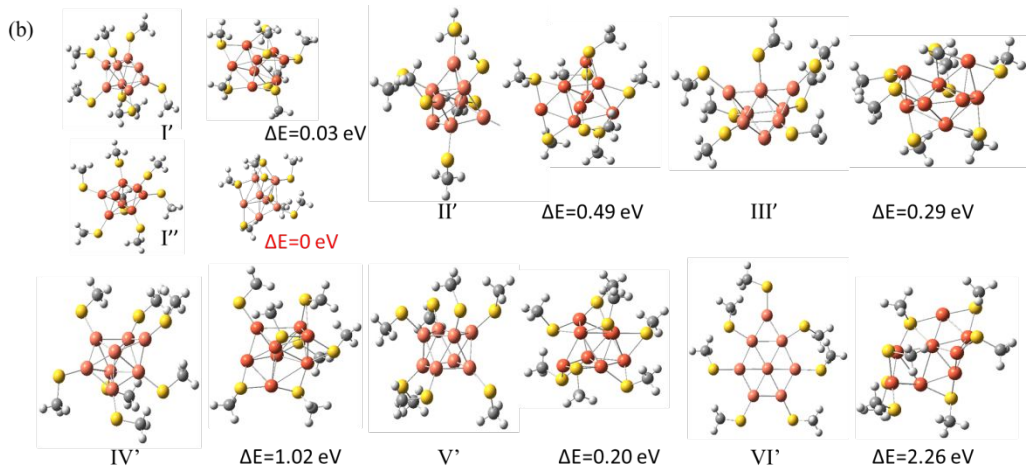

Figure S3. (a) Possible calculated isomers of Cu_8 core and (b) $Cu_8(SG)_7$ before (I-VI, I'-VI') and after optimization.

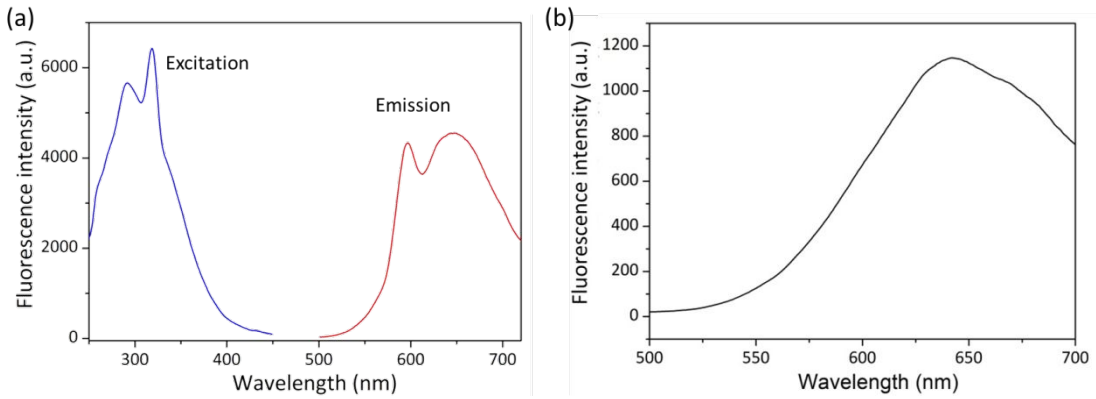

Figure S4. (a) Photoluminescence of Cu_8 NCs, emission (red) and excitation (blue) spectra. (b) Fluorescence spectrum of Cu NCs when excited in 370 nm.

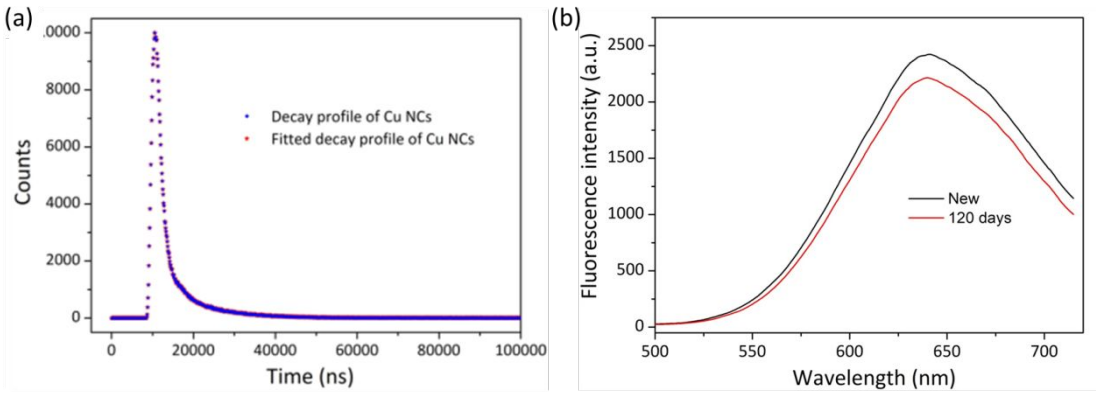

Figure S5. (a) Time-resolved fluorescence decay profile of Cu_8 NCs, (b) Fluorescence spectra of Cu NCs in different time (λex=370 nm).

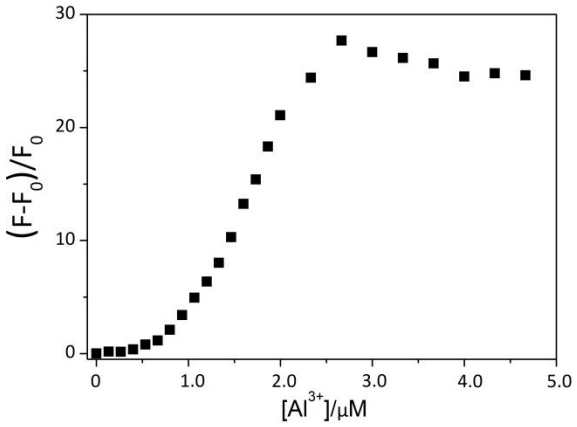

Figure S6. The emission intensity of Cu NCs with the Al^{3+} ions increasing monitored at 645nm with λ_{ex}= 370 nm.

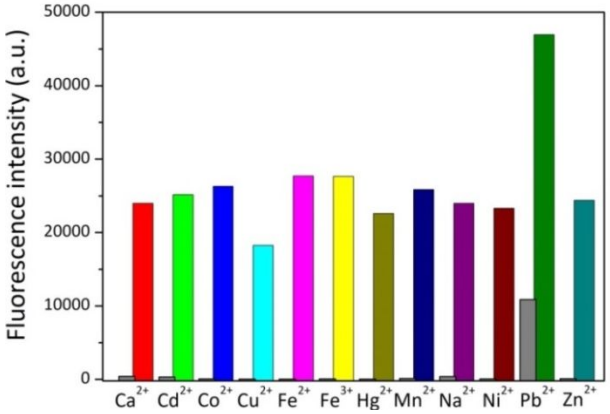

Figure S7. Competitive experiments of Cu_8 NCs with Al^{3+} in the presence 1.0 equiv of various metal ions at 645 nm. Gray bars: Cu_8 NCs with metal ions stated. Colored bars: solutions of Cu NCs with Al^{3+} and other ions stated.

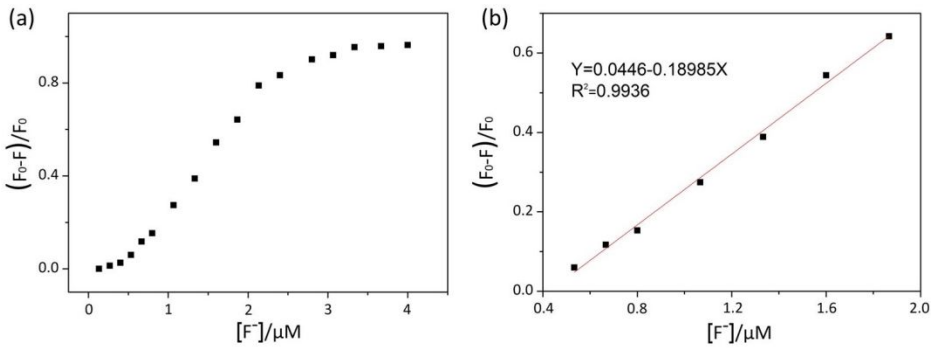

Figure S8. (a) The emission intensity of Cu_8 NC-Al^{3+} with F^- increasing monitored at 645nm with λ_{ex}= 370 nm. (b) The linear detection range for F^-.

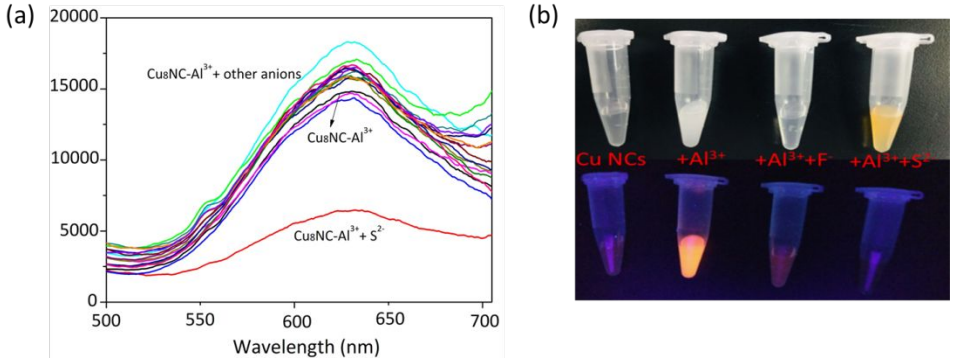

Figure S9. (a) Fluorescence responses of Cu NC-Al^{3+} with various anions monitored at 645nm with λ_{ex}= 370 nm. (b) Photo images of Cu NCs in the absence and presence of Al^{3+}, S^{2-} and F^- ions.

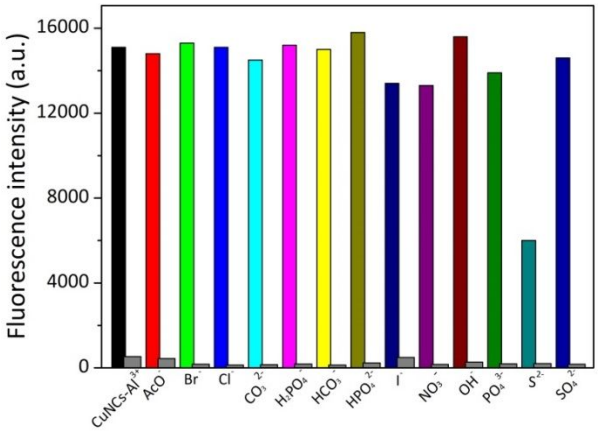

Figure S10. Competitive experiments of Cu_8 NC-Al^{3+} in the presence 1.0 equiv of various anions at 645 nm. Colored bars: solutions of Cu_8 NC-Al^{3+} and 1.0 equivalent of the other anions stated. Gray bars: Cu NC-Al^{3+} in the presence of F^- ions with other anions stated.

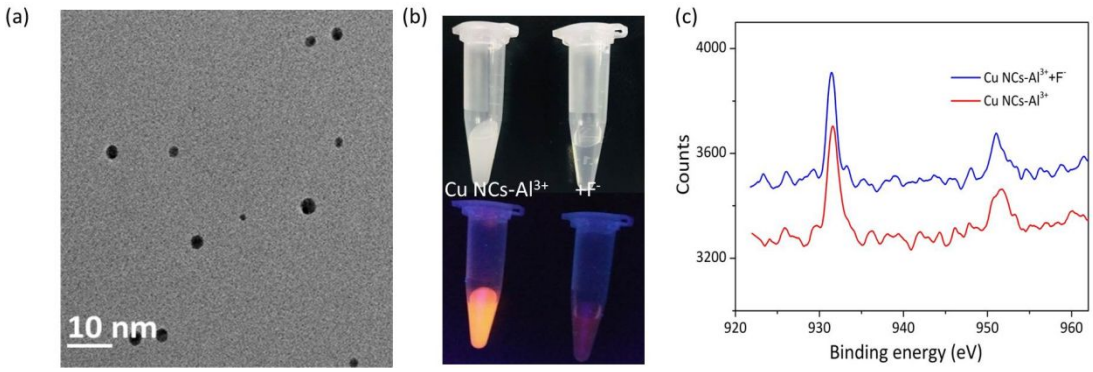

Figure S11. (a) TEM image of Cu NC-Al^{3+} ensemble after adding F^- ions. (b) Photo images of Cu NC-Al^{3+} ensemble in the absence and presence of F^- ions. (c) XPS spectra of Cu 2p for the Cu NC-Al^{3+} ensemble in the presence F^- ions.

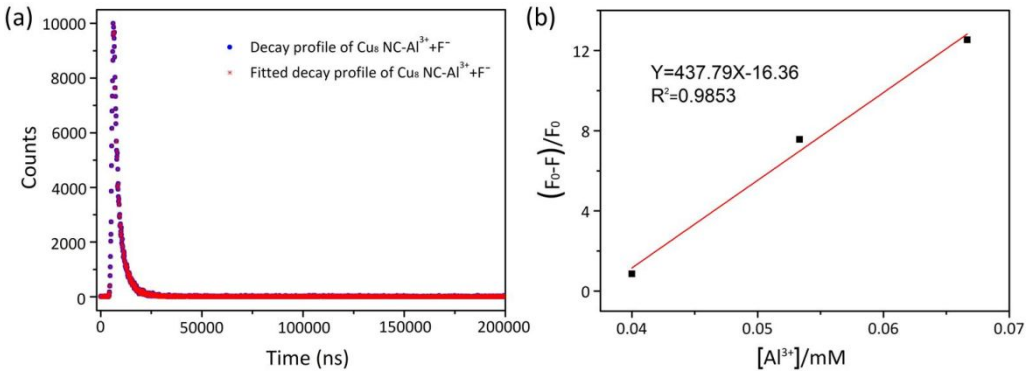

Figure S12. (a) The fluorescence decay profile of Cu_8 NC-Al^{3+} upon the addition of F^-. (b) The linear detection range for Al^{3+}.

Table S1. Comparison of fluorescence methods for the detection of F^- in various solvent and the LOD.

Methods	Solvent	LOD (μM)	Ref.
$[Eu.L^{1\text{-}2}]^+$	H_2O	0.2–50 μM	6
DL-PQDs	toluene	3.2	14
QD-conjugate	$CHCl_3$	0.74	15
Schiff base	DMSO	70	16
NIM	DMSO	14.36	17
LMOFs	DMF/H_2O	2.0	21
Cu_8 NC-Al^{3+}	H_2O	0.16	This work